GeoVirtual 2020 September 14-16
Resilience and Innovation

IMPACT OF SEISMIC HAZARD ON THE GROUND RESPONSE IN EASTERN NORTH AMERICA

Huo-Kang, J. & Yniesta, S.
Department of Civil, Geological and Mining Engineering,
Polytechnique Montreal, Montreal, Qc, Canada

ABSTRACT
In practice, dynamic nonlinear simulations are performed by selecting ground motions to match the uniform hazard spectrum (*UHS*) over a period range, for a pair of magnitude and distance (*M-R*). The latter are being picked based on a deaggregation analysis. The selection of the seismic scenario and the period range over which the ground motions are scaled, has a significant impact on the selection of ground motions, and the results of the simulations. In Eastern North-America (*ENA*), ground motion selection is further complicated by the lack of well-recorded ground motions at *M-R* of interest. This paper discusses the influence of the selection of the seismic hazard scenarios on the wave propagations in a soil profile. Dynamic non-linear simulations are conducted for six scenarios. The results obtained are compared in terms of response spectra, level of amplification, acceleration profile, and factor of safety to liquefaction, to determine the impact of the selection of seismic scenarios on the propagation of seismic waves.

RÉSUMÉ
Dans la pratique, les analyses dynamiques nonlinéaires sont réalisées en sélectionnant des accélérogrammes correspondant au spectre d'aléa uniforme (*UHS*) sur la plage de période considérée, pour une paire *M-R*. Les paires *M-R* sont choisies en se basant sur l'analyse de la déaggrégation. La sélection des scénarios a un impact significatif sur la sélection des accélérogrammes et, donc, sur les résultats des simulations. Dans le nord-est américain, la sélection des accélérogrammes est d'autant plus difficile à cause du manque d'accélérogrammes historiques enregistrés pour les paires *M-R* d'intérêt. Cet article discute de l'influence de la sélection des scénarios sismiques sur le comportement dynamique d'un profil de sol. Des analyses dynamiques nonlinéaires ont été réalisées pour six scénarios sismiques. Les scénarios sont comparés en termes de réponse spectrale, du niveau d'amplification, du profil d'accélération et de la prédiction à la liquéfaction; le but étant de déterminer l'impact de la sélection des scénarios sismiques sur la propagation des ondes sismiques.

1 INTRODUCTION

Time history dynamic analyses require definition of the seismic hazard within the design period range. The latter generally corresponds to periods in which the majority of inelastic deformations take place. Input ground motions must be selected in accordance to the seismic hazard and the seismic scenario (i.e. a pair of magnitude and distance) that dominates the hazard. To define the seismic scenario, analysis of the deaggregation of the region must be performed. The objective is to deaggregate the seismic hazard in order to retrieve the principal contribution of earthquake sources in terms of magnitude and distance. Scenarios of magnitude and distance (*M-R*) are established for the entire design period range.

In Eastern North America (*ENA*), it is widely accepted that at short periods, seismic hazard is dominated by events of low magnitudes and short distances while at long distances, events of high magnitudes and long distances dominate (Atkinson, 2009). Hence, Atkinson (2009) suggests using 2 scenarios to represent the seismic hazard. In general, 3 scenarios should be enough to adequately represent the design period range (Tremblay et al, 2015). The definition of scenarios is an important step due to its influence on the selection of input ground motions, and the subsequent analysis.

The objective of this article is to analyze the impact of the seismic hazard and the different scenarios considered on the propagation of seismic waves throughout a soil column. The soil layers are defined based on available geotechnical information and using empirical relationships to define the dynamic properties. Based on the analysis of the deaggregation of the seismic hazard, seismic scenarios are established for the entire design period range. Selection of input ground motions is performed based on several selection criteria and are then scaled to match the target response spectrum $S_T(T)$. Compatibility of ground motions with the $S_T(T)$ is discussed. Finally, nonlinear ground response analyses are performed using the software DEEPSOIL. The results with each scenario are compared in terms of seismic amplification, acceleration profile, and contribution to the liquefaction hazard.

2 SOIL PROFILE

The studied soil profile is located in Montreal, QC, Canada, and is composed of a thin layer of gravel and sand, a layer of compacted silt overlaying a layer of loose silt as illustrated in Figure 1. The bedrock is located at a depth of 21.9 m, and coring in the bedrock indicates high quality with an RQD above 90. Based on local knowledge of the geology, the rock is considered stiff, corresponding to a class NEHRP class A (Finn and Wightman, 2003; NEHRP, 1994).

Several Standard Penetration Test (*SPT*) borings and a multichannel analysis surface wave (*MASW*) survey were performed at the site, and piezometers were installed in geotechnical borings. The measured shear wave velocity profile (V_s) is presented in Figure 1. Based on the V_s profile the natural period (T_1) of the soil column was computed as 0.38 s.

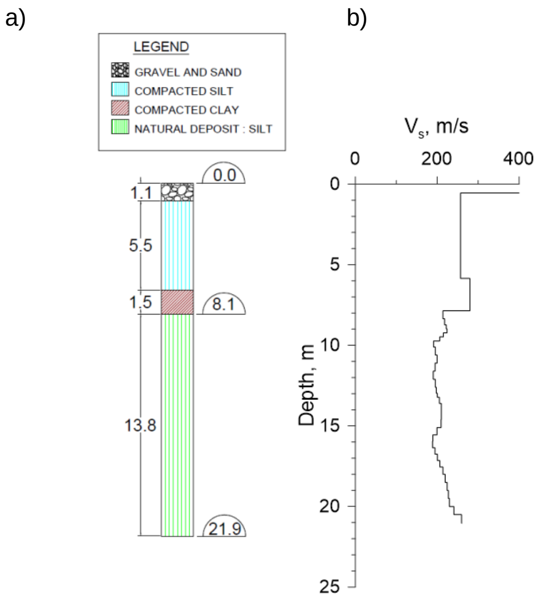

Figure 1. a) Boring log b) Shear wave velocity (V_s) profile

3 SEISMIC HAZARD

This section discusses the seismic hazard for a 2 % in 50 years (i.e. a 2475-year return period) probability of occurrence in the region of Montreal, QC, Canada. Deaggregation analysis provided by the Canadian Geological Survey is first studied to determine the main contributions to the uniform hazard spectrum (*UHS*) in terms of pairs of magnitudes and distances. Then, seismic scenarios consistent with the $S_T(T)$ are selected.

3.1 Target response spectrum $S_T(T)$

The NBCC 2015 defines the $S_T(T)$ as a *UHS* based on a probabilistic seismic hazard analysis (*PSHA*). As such the spectrum has a uniform probability of occurrence, although it is composed of contributions of multiple sources and considers several scenarios for a given seismic source. Hence the spectrum is not representative of a single event and is not a realistic spectrum (Baker, 2011).

The $S_T(T)$ is provided by The Geological Survey of Canada and is computed from the online hazard tool (https://earthquakescanada.nrcan.gc.ca/index-en.php). The *UHS* is originally computed for a site of seismic class C and spectral acceleration are provided for *PGA* and periods 0.05, 0.1, 0.2, 0.3, 0.5, 1.0, 2.0, 5.0 and 10 s. The spectrum is then modified with period-dependent site coefficients *F(T)* provided by the NBCC 2015 and based on the study of Finn and Wightman (2003), to obtain the seismic hazard at the top of the rock, the latter being considered of class A, as mentioned above. The obtained design spectrum is presented in Figure 2.

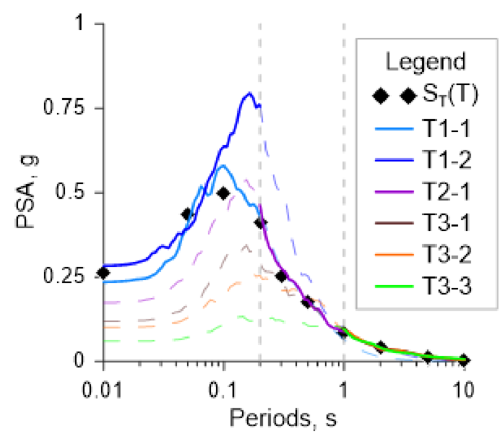

Figure 2. Target Response Spectrum $S_T(T)$ and average spectrum scaled to $S_T(T)$ within specific-scenario period range T_{RS}

3.2 Deaggregation analysis

A seismic hazard deaggregation analysis provides the relative contribution of each earthquake source to the hazard in terms of magnitudes and distances (Bazzurro and Cornell, 1999; Halchuk et al., 2019; Kramer, 1996). The deaggregation of Montreal was provided from the Canadian Geological Survey for the *PGA* and periods 0.1, 1.0, and 5.0 s is presented in Figure 3. It should be noted that the current version of the NBCC does not provide epsilon in their deaggreagation studies, and therefore this parameter is omitted in the current study.

For the purpose of this project, the target period range (T_R) considered for spectral acceleration ranges between 0.01 and 10 s, which what is being typically provided by

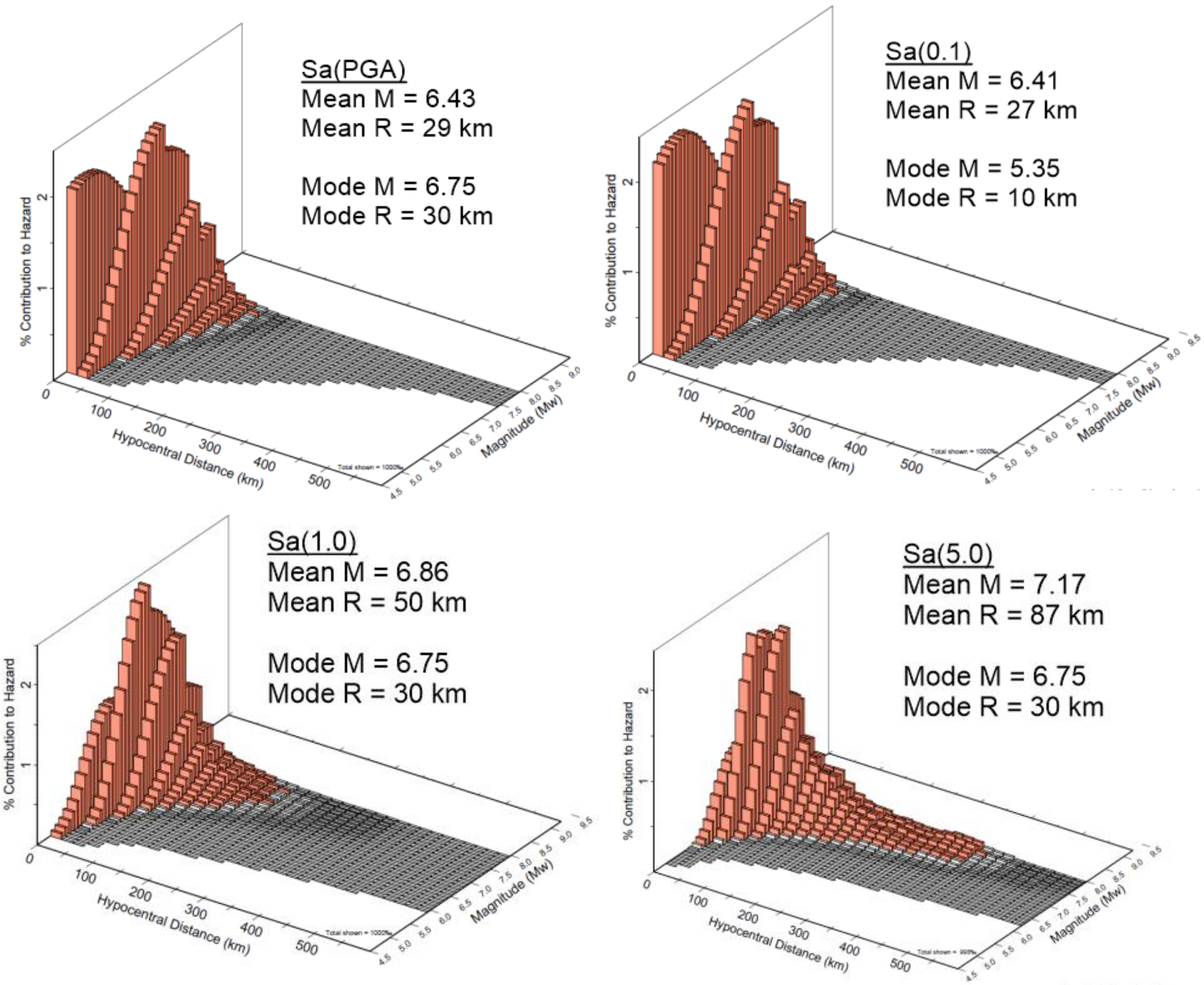

Figure 3. Deaggregation of Montreal for a probability of 2% for 50 years for the *PGA* and periods 0.1, 1.0, 5.0 s

building codes. In *ENA*, it is generally accepted that the seismic hazard is dominated by events of low magnitudes and short distances at short spectral periods, and of high magnitudes and long distances at long periods (Atkinson, 2009; Halchuk et al., 2019). However, the deaggregation shows that the seismic hazard in Montréal is not bimodal, but rather has a wide distribution and that a few earthquake scenarios might be more representative. In this study, we study the contributions of a few scenarios to different period ranges of the hazard. The hazard spectrum is divided into 3 period ranges; from 0.01 to 0.2 s, 0.2 to 1.0 s and 1.0 to 10 s. For each period range, the most likely scenarios are identified based on the deaggregation.

In addition to the seismic scenarios suggested by Atkinson, 2009 in *ENA*, seismic events of high magnitudes and medium distances (M6-7 and R20-40 km) contribute significantly to the hazard at short periods (T1-2), hence two scenarios are selected.

At medium periods, only one scenario controls the hazard. For long periods, events at short distances (R20-40 km) also have a non-negligible contribution to the hazard. Which led to the selection of three scenarios. All scenarios are presented in Table 1.

Table 1. Seismic scenarios considered in the present study.

Scenario	Scenario-specific period range T_{RS} (s)	Magnitude R	Fault-distance R (km)
T1-1	0.01 – 0.2	5 – 6	0 – 20
T1-2	0.01 – 0.2	6 – 7	20 – 40
T2-1	0.2 – 1.0	6 – 7	20 – 40
T3-1	1.0 – 10	6.5 – 7.5	20 – 40
T3-2	1.0 – 10	7 – 7.5	40 – 60
T3-3	1.0 – 10	7 – 7.75	70 – 130

4 SELECTION AND SCALING OF INPUT GROUND MOTIONS

The goal of this paper is to study, through the use of ground response analysis, how the soil profile amplifies or attenuates the propagation of seismic waves based on different seismic scenarios representative of different parts of the spectrum. In this section, the selection and scaling of input ground motions consistent with each scenario are discussed.

4.1 Selection of input ground motions

Historical ground motions are used as input motions in the ground response analyses. Recordings were primarily selected to be consistent with the distances and magnitudes of each relevant scenario. A secondary criterion was to select recordings on stiff rock when possible. Since the number of recorded strong motions in *ENA* is low, both the NGA-East (Goulet et al. 2018) and the NGA-West2 (Ancheta et al. 2013) databases were used to look for ground motion recordings. NGA-West 2 contains a wide set of motions recorded worldwide, while NGA-East is more limited and contains motions recorded in Central and Eastern North America.

Selection and scaling of ground motions are performed based on the NBCC 2015 Commentary J Guidelines. The principal selection criteria were as follows:

1. Eleven ground motions per scenario
2. A scaling factor (F_1) between 0.5 and 2.0, computed based on the SIa scaling method such that the area under the record spectrum equals the area under the $S_T(T)$ over the scenario-specific period range T_{RS} (see the next section).
3. A shape similar to the $S_T(T)$ within the T_{RS}
4. Shape outside T_{RS} falls below the $S_T(T)$
5. The mean computed spectrum of the recorded motions (S_g) does not fall below 75 % of the S_T(T) outside T_{RS}.
6. No more than 2 records from the same earthquake
7. The mean S_g does not fall below 90 % of the $S_T(T)$ within T_{RS}. A second scaling factor (F_2) is applied to adjust the average spectrum S_g if necessary.

4.2 Scaling of input ground motions

Ground motions are scaled using SIa scaling method which applies a scaling factor F_1 to the record. It scales the motions such that the area under the record spectrum equals the area under the $S_T(T)$ within the T_{RS}. A recent study realized in *ENA* has shown reliable results in terms of peak ground motion (*PGA*) and arias intensity (*AI*) using the SIa scaling method (Michaud and Léger, 2014). In preference, the F_1 should be kept as close to 1 as possible (Krinitsky and Chang, 1979). Limits of 0.5 to 2.0 to F_1 are appropriate when the records are selected based on the magnitude, the distance and the site conditions (Watson-Lamprey and Abrahamson, 2005).

It is important that the ground motion does not exceed the $S_T(T)$ outside T_{RS}, otherwise, the benefits of using multiple scenarios are cancelled. The scaled selected ground motions are presented in Figure 4 for each scenario. Note that Figure 2 also provides the mean S_g for each scenario. Table 2 presents some of the characteristics of the motions selected for each scenario including the average *PGA*, the average *AI*, the average shear-wave velocity of the uppermost 30 m soil layer (V_{s30}), the average F_1 and the average F_2.

4.3 Compatibility issues

Figure 4 shows that the shape of S_g within the T_{RS} was the most limiting selection criterion for T1-1 and T1-2. In general, the S_g falls well under $S_T(T)$ below 0.05 s and well above $S_T(T)$ above 0.05 s, especially for T1-2. This leads to an acceptable scaling factor F_1 but a poor match between S_g and $S_T(T)$.

Selection of ground motions was especially difficult for scenario T1-2 which represents M6-7 and R20-40 km between periods 0.01 and 0.2 s. Since the database NGA-East does not contain ground motions corresponding to this M-R scenario, only the database NGA-West 2 was used for this scenario. The shape of the average spectrum S_g matches poorly the $S_T(T)$ within T_{RS} (Figure 4). In fact, the peaks of individual spectrum are generally shifted to longer periods leading to pseudo-spectral acceleration (*PSA*) being lower at short periods. The mean S_g exceeds the $S_T(T)$ outside T_{RS}, and the *AI* is higher compared to the other scenarios, which may result in an exaggerated dynamic response.

Scenario T2-1 offers acceptable compatibility with the $S_T(T)$ within T_{RS}, while the mean S_g of scenarios T3-1 to T3-3 correctly match the $S_T(T)$ within T_{RS} but are well below $S_T(T)$ at shorter periods.

The NBCC 2015 recommends that S_g after scaling does not drop below 75% of the $S_T(T)$ outside T_{RS}. Unfortunately, few to no ground motion corresponding to scenarios T3-1 to T3-3 respect this criterion, further supporting that the design spectrum is unrealistic. As a result, the *PGA* for these scenarios is much lower than the design values.

However, for the purpose of this exercise, the authors found interesting the study of a scenario of a large magnitude earthquake located at a far distance, and how it might affect the design.

As a conclusion, historical ground motions recorded in other regions seem to have limited compatibility with the seismic hazard in *ENA* at short and long periods since their shape do not match.

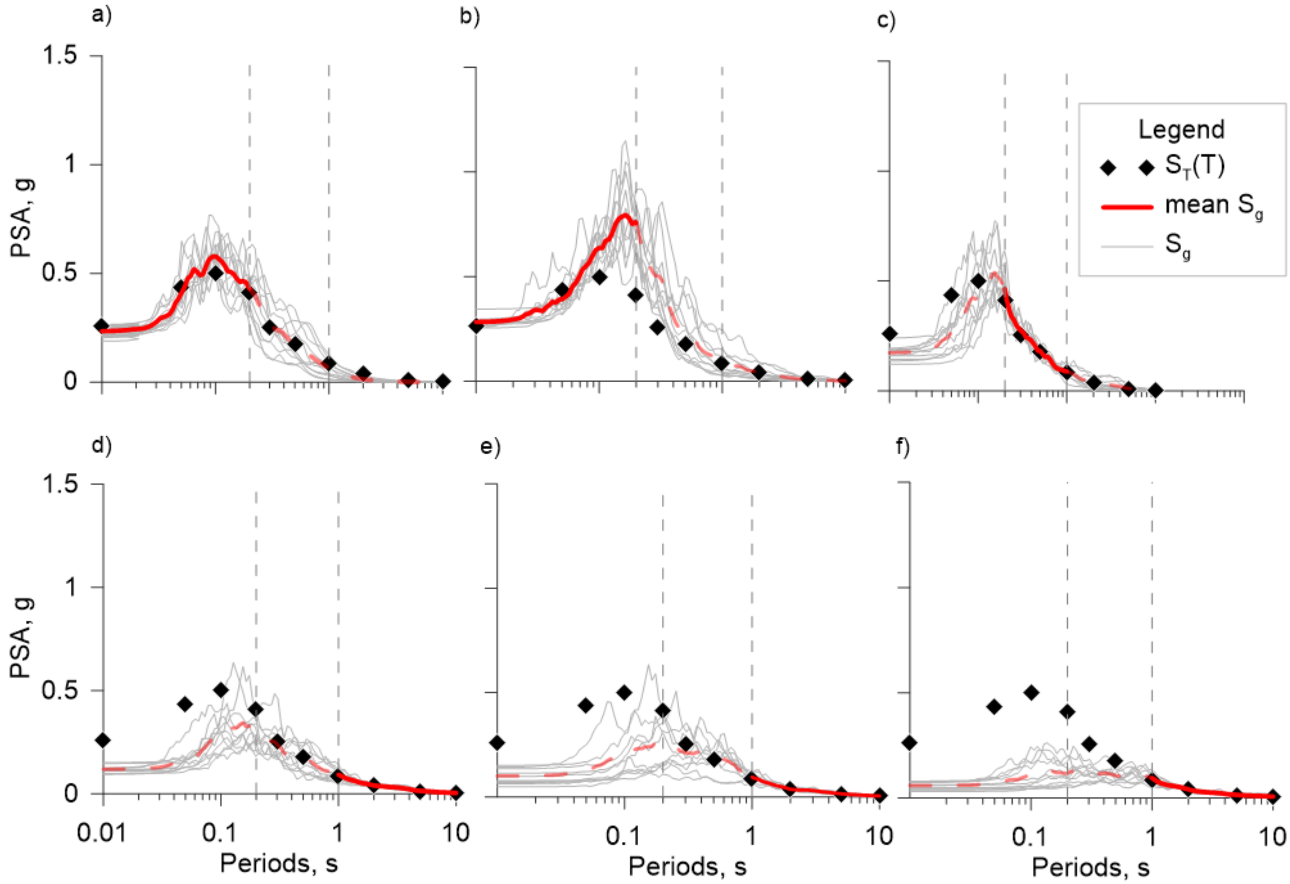

Figure 4. Input grounds motions of scenario a) T1-1, b) T1-2, c) T2-1, d) T3-1, e) T3-2 and f) T3-3

Table 2. Selected input motions per scenario with average peak ground acceleration (*PGA*), average arias intensity (*AI*), average shear wave velocity at the uppermost 30 m soil layer (V_{s30}), average scaling factor (F_1) and average second scaling factor (F_2).

Scenario	PGA (g)	AI (m/s)	V_{s30} (m/s)	Scaling factor F_1	Second scaling factor F_2
T1-1	0.235	0.386	674	1.34	1.04
T1-2	0.283	1.50	560	1.29	1.27
T2-1	0.174	0.676	594	1.17	1.00
T3-1	0.119	0.440	575	1.23	1.00
T3-2	0.101	0.415	605	1.33	1.03
T3-3	0.060	0.165	655	1.59	1.00

5 INPUT PARAMETERS FOR GROUND RESPONSE ANALYSIS

Nonlinear ground response analyses are performed using the software DEEPSOIL v.6.1 (Hashash et al. 2016). The soil profile is discretized in layers thin enough to propagate a 75 Hz frequency. The necessary input parameters of each layer include the unit weight (γ), estimated based on available geotechnical data, the shear wave velocity (V_s), and modulus reduction and damping curves. The measured V_s profile is presented in figure 1b. The analyses are ran using the General Quadratic/Hyperbolic Strength-Controlled constitutive model (*GQ/H*) (Groholski et al. 2016), which also requires the shear strength S_u.

The modulus reduction and damping curves are defined by the empirical relationships developed by Darendeli (2001). The empirical model requires the plasticity index (*PI*) and the overconsolidation ratio (*OCR*). Since no characterization tests were performed on the clayey materials a typical value for Champlain clays of *PI*=30 is assigned, and an *OCR* of 2.5 is assigned given its compacted state. The small strain damping is introduced using the frequency-independent damping scheme (Phillips and Hashash 2009).

The *GQH* defines the backbone curve as a combination of the stress-strain curve induced by the input modulus reduction curve at low strains, and the S_u defined by the user at large strains. The target S_u is defined based on the SHANSEP concept for coherent soils based on Ladd and Foott (1974), and Mohr-Coulomb criteria for noncoherent soil as defined by equations 1 and 2 respectively. The friction angle (ϕ) is calculated based on the results of *SPT* tests, σ_v and σ'_v are the confining pressure and effective confining pressure respectively.

$$S_u = 0.22 OCR^{0.8} \sigma'_v \quad [1]$$

$$S_u = \sigma_v tg(\phi) \quad [2]$$

6 ANALYSIS OF THE RESULTS

One dimensional nonlinear ground response analyses are performed for each scenario, and the input motions are applied at the base of soil column, i.e. the top of the bedrock.

Figure 5 shows the average *PGA* profile through the soil column for all scenarios. Motions scaled for the medium and long period ranges, i.e. T2 and T3, amplify the *PGA*, while short period ranges (i.e. T1), attenuate the *PGA*. This is in accordance with the principle that low *PGA* are typically amplified, while high *PGA* are attenuated (Idriss, 1990). Indeed, seismic waves tend to get trapped in the soft layers due to large impedance contrast with subsequent layers and the underlying bedrock and thus the interference of trapped waves would further lead to resonance in the soft layers. Idriss (1990) has found that rock motions below a *PGA* of 0.1 g would produce high amplification ratios, in the range of 1.5 – 4.0, when the response is nearly elastic. Increase of non-linearity of soft soil sites due to higher *PGA* reduces the amplification ratios because of the increase of hysteretic damping and decrease of shear modulus.

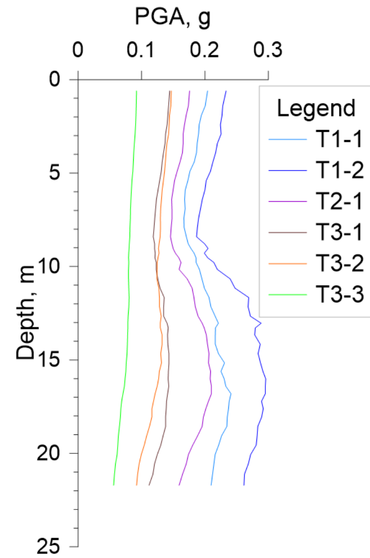

Figure 5. PGA profile

This amplification effect is further confirmed by studying the spectral amplification, i.e. the ratio of surface to input spectral acceleration, as shown in Figure 6. It is interesting to note that amplification at the degraded natural period T_1 (0.68 s) is of similar level between all scenarios, but that for low periods the amplification is more highly dependent on the input motion. Note that the current soil amplification factors of the NBCC 2015 would not be able to capture this effect.

Since amplification is observed in the middle of the loose silt layer which is susceptible to liquefaction, it is interesting to evaluate its liquefaction potential. The factor of safety for liquefaction is computed for each scenario over depth and is presented in Figure 7. The factor of safety is computed as the ratio between cyclic resistance ratio (*CRR*) and cyclic stress ratio (*CSR*) both computed based on the procedure described by Boulanger and Idriss (2014).

Liquefaction potential prediction is quite different between scenarios. Only scenarios T1-2 and T2-1 indicate liquefaction in the loose silt layer with a factor of safety below 1. While the scenario T1-2 is the scenario with the highest *AI* and *PGA*, and might be associated with difficulties with selection and scaling as explained above, the scenario T2-1 has a lower *PGA*, and the *PGA* profile is lower than scenario T1-1. However, since the magnitude is greater, the potential for liquefaction is also greater.

This further suggests that multiple possible scenarios ought to be considered when evaluating the potential for liquefaction in practice, even though scenarios not controlling the *PGA*, because they can contribute to the probability of liquefaction. It is therefore recommended that liquefaction be studied in a probabilistic manner rather than the more spread-out deterministic approach.

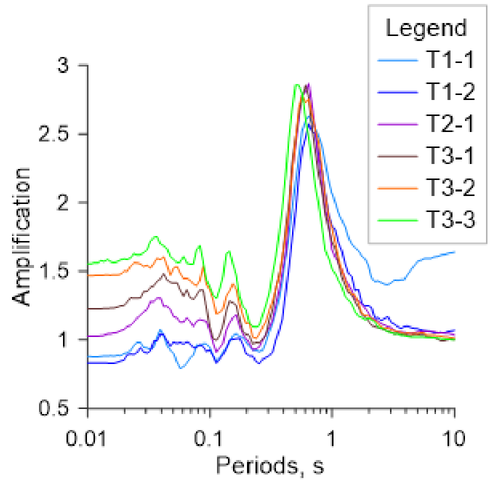

Figure 6. Amplification at the crest

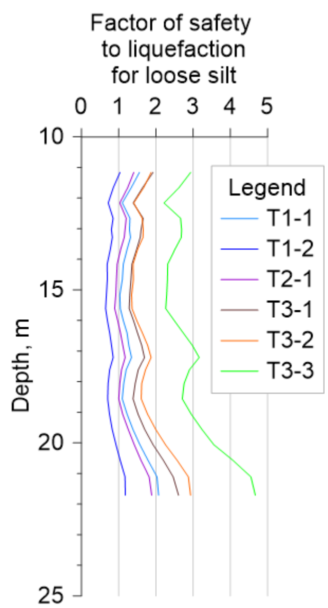

Figure 7. Factor of safety to liquefaction vs. depth in the loose silt layer.

7 CONCLUSION

In this article, nonlinear 1D dynamic analyses are performed on a soil profile using software DEEPSOIL. Prior to analyses, the seismic hazard is defined by analyzing the results of the deaggregation in the region of Montreal, QC, Canada. Relative contribution of earthquake sources in terms of magnitude and distance are analyzed and seismic scenarios are established. As the design period range is considered to span from 0.01 to 10 s, a total of six scenarios are selected to define the spectrum. Two scenarios are needed at short periods between 0.01 and 0.2 s (T1-1 and T1-2), one scenario between 0.2 and 1.0 s (T2-1) and three scenarios between 1.0 and 10 s (T3-1 to T3-3). Input ground motions are selected and scaled to match the target response spectrum $S_T(T)$ within the scenario-specific period range T_{RS}.

Here are the principal observations:

- Historical ground motions generally do not match the shape of $S_T(T)$ at short periods (T1-1 and T1-2). Thus, for short natural period embankments, compatibility issues with the $S_T(T)$ can become problematic especially because the seismic behavior of small embankments is highly influenced by the selection of ground motions.
- At long periods (T3-1 to T3-3), it was difficult to impossible to keep a minimum of 75% of the $S_T(T)$ outside the T_{RS} as recommended by the NBCC 2015.
- The loose deposit has a potential for liquefaction, and this potential is controlled by motions that affect both short and medium periods. Thus, considering multiple scenarios for the evaluation of liquefaction is beneficial.
- The *PGA* is amplified for long period motions, because they are associated with a low input *PGA*. On the contrary, higher input *PGA* are attenuated in the soil profile. This induces that low input *PGA* might also contribute to the risk of liquefaction, although in the present study, the factor of safety remained high.

8 REFERENCES

Ancheta, T., D., Darragh, R. B., Stewart, J. P., Seyhan, E., Silva, W. J., Chiou, B. S. J., Wooddell, K. E., Graves, R. W., Kottke, A. R., Boore, D. M., Kishida, T. and Donahue, J. L. 2013. PEER NGA-West2 Database, *Pacific Earthquake Engineering Research Center*, California, CA, United States.

Atkinson, G. M. 2009. Earthquake time histories compatible with the 2005 National building code of Canada uniform hazard spectrum, *Canadian Journal of Civil Engineering*, 36(6): 991-1000.

Baker, J. W. 2011. Conditional Mean Spectrum: Tool for ground motion selection, *Journal of Structural Engineering*, 137(3): 322-331.

Boulanger, R. W., & Idriss, I. M. (2014). CPT and SPT based liquefaction triggering procedures. *Report No. UCD/CGM.-14,* 1:1-138.

Bazzurro, P. & Cornell, C. A. 1999. Disaggregation of seismic hazard. *Bulletin of the Seismological Society of America*. 89(2): 501-520.

Darendeli, M. B. 2001. Development of a new family of normalized modulus reduction and material damping curves. PhD thesis. *The University of Texas at Austin*. Austin, Texas, United States.

Finn, W. L., & Wightman, A. 2003. Ground motion amplification factors for the proposed 2005 edition of the National Building Code of Canada, *Canadian Journal of Civil Engineering*, 30(2): 272-278.

Goulet, C., Bozorgnia, Y., Abrahamson, N., Kuehn, N., Atik, L. A., Youngs, R., Graves, R. and Atkinson, G. 2018. Central and Eastern North America Ground-Motion Characterization – NGA-East Final Report, *Pacific Earthquake Engineering Research Center*, California, CA, United States.

Groholski, D. R., Hashash, Y. M. A., Musgrove, M., Harmon, J. & Kim, B. 2015. Evaluation of 1-D Non-linear site response analysis using a General Quadratic/Hyperbolic strength-controlled constitutive model, *6th International Conference on Earthquake Geotechnical Engineering*, Christchurch, New Zealand.

Halchuk, S., Adams, J., & Kolaj, M. & Allen, T. 2019. Deaggregation of NBCC 2015 Seismic Hazard for Selected Canadian Cities, *12th Canadian Conference on Earthquake Engineering*, Quebec City, QC, Canada.

Hashash, Y. M. A., Musgrove, M. I., Harmon, J. A., Groholski, D. R., Phillips, C. A. & Park, D. 2016. "*DEEPSOIL V 6.1., User Manual*", University of Illinois at Urbana-Champaign, Urbana, Illinois.

Idriss, I. M. 1990. Response of soft soil sites during earthquakes, *H. Bolton Seed Memorial Symposium*, Berkeley, California, United States, 2: 273:289.

Kramer, S. L. 1996. *Geotechnical earthquake engineering*, Prentice Hall, Upper Saddle River, N. J., United States.

Krinitzsky, E. L. & Chang, F. K. 1978. State-of-the-art for assessing earthquake hazards in the United States: Specifying peak motions for design earthquakes. *U. S., Army Engineer Waterways Experiment Station Soils and Pavements Laboratory*, United States.

Ladd, C. C. & Foott, R. 1974. New Design Procedure for Stability of Soft Clays, *Journal of Geotechnical and Geoenvironmental Engineering*, 100: 763-786.

Michaud, D., & Léger, P. 2014. Ground motions selection and scaling for nonlinear dynamic analysis of structures located in Eastern North America, *Canadian Journal of Civil Engineering*, 41(3): 232-244.

NEHRP. 1994. 1994 Recommended provisions for seismic regulations of new buildings: Part 1, provisions. FEMA 222A, *National Earthquake Hazard Reduction Program*, *Federal Emergency Management Agency*.

NRC. 2015. National Building Code of Canada. *National Research Council*. Ottawa, ON, Canada.

Pacific Earthquake Engineering Research (PEER). 2010b. Technical report for the PEER ground motion database web application [online]. Available at http://peer.berkely.edu/peer_ground_motion_database

Phillips, C. & Hashash, Y. M. A. 2009. Damping formulation for nonlinear 1D site response analyses, *Soil Dynamics and Earthquake Engineering*, 29: 1143-1158.

Tremblay, R., Atkinson, G. M., Bouaanani, N., Daneshvar, P., Léger, P., & Koboevic, S. 2015. Selection and scaling of ground motion time histories for seismic analysis using NBCC 2015. *11th Canadian Conference on Earthquake Engineering*, Victoria, BC, Canada.

Watson-Lamprey, J. & Abrahamson, N. 2005. Selection of ground motion time series and limits on scaling, *Soil Dynamics and Earthquake Engineering*, 26(5): 477-482.